
# Neutron Moderation in ICF Pellets and Effects on Damage and Radioactive Inventory

F. Beranek and R.W. Conn

May 1979

UWFDM-310

FUSION TECHNOLOGY INSTITUTE

UNIVERSITY OF WISCONSIN

MADISON WISCONSIN

# Neutron Moderation in ICF Pellets and Effects on Damage and Radioactive Inventory

F. Beranek and R.W. Conn

Fusion Technology Institute
University of Wisconsin
1500 Engineering Drive
Madison, WI 53706

http://fti.neep.wisc.edu

May 1979

UWFDM-310

# Neutron Moderation in ICF Pellets and Effects on Damage and Radioactive Inventory

F. Beranek*
R.W. Conn

Fusion Engineering Program
Nuclear Engineering Department
University of Wisconsin

May 1979

UWFDM-310

* Presently with E.I. du Pont de Numours & Co.
Savannah River Plant
Aiken SC 29801

## Abstract

A standard time dependent neutron transport computer code, TDA, is modified to allow time varying material density in order to calculate the neutron spectrum from exploding inertial confinement fusion (ICF) pellets with $\rho R$ values of 0 to 6 g/cm$^2$. Softening of the spectra due to neutron-fuel interactions causes a time-of-flight broadening of the neutron arrival time distribution at the chamber wall. It is found that the total number of displacements per atom produced in a graphite first wall increases with the $\rho R$ of the pellet over the $\rho R$ range investigated because the dpa cross section is larger at lower neutron energy. However, the total helium production decreases with increasing $\rho R$ as does the peak damage rate. Neutron induced radioactivity generated in a 10 mg iron tamper is of the same magnitude as that produced in the rest of an entire reactor system.

## I. Introduction

An inertial confinement fusion (ICF) pellet in a compressed state, though absolutely very small, is an extremely dense medium composed primarily of light elements (e.g. deuterium and tritium). The super-high density means there is a substantial collision probability for fusion neutrons created in the pellet. Compounding the moderation effect is the large energy loss per elastic scattering event. As a consequence, one might expect a significantly softer neutron spectrum coming from such a target and a concomitant reduction in the peak instantaneous damage rates incurred by the first wall of the reactor vessel. In addition to the fuel, a pellet may be constructed such that its outermost layer is composed of a high Z material which plays the role of a tamper. The optically thin outer skin will experience an extremely large neutron flux which can result in a significant production of radioactive isotopes. This must be considered in assessing the gas handling system of a reactor and the disposal of activated components.

Several methods to calculate the neutron spectra from ICF targets have been reported. F.H. Southworth and J.O. Campbell used collision probability theory to generate the spectrum.[1] Using the Wigner Rational Approximation, the escaping flux is determined as the sum of the uncollided flux and the first and second collided fluxes. They note that 20% of the neutrons are downscattered in an equimolar DT pellet with $\rho R = 2$ g/cm$^2$. (ICF pellets are often characterized by the term $\rho R$, the product of the pellet density and the radius in the compressed state.) Various assumptions are inherent in a calculation of this type such as the assumptions that the pellet density and neutron source are both spatially uniform and time independent and that

the interaction cross sections are energy and angle independent.

A Monte Carlo code, SPECIFIC II, has been used by T.D. Beynon and G. Constantine to generate a spectrum from a pellet with $\rho R = 1.2$ g/cm$^2$.[2] The result for this case, employing a steady-state technique with a uniform source, is that less than 1% of the neutrons are downscattered.

Some effects of neutron moderation in an ICF pellet are described in a report by J.A. Blink, et al.[3] Their studies involve an examination of integral parameters characterizing blanket performance. They illustrate that the softer neutron spectrum causes a decrease in the blanket tritium breeding ratio but an increase in the blanket energy multiplication factor.

We present here neutron pellet spectra obtained using a modified form of the time dependent discrete ordinate code, TDA.[4] The spatial profiles of the neutron source and pellet density are allowed to be both non-uniform in space and time dependent. The interaction cross sections are energy dependent (multi-group) and anisotropic. Neutron damage to a reactor chamber, both time dependent and time integrated, is shown to be significantly altered when moderation in the pellet is included. The potential radioactivity inventory problem caused by an iron tamper is also demonstrated.

## II. Theory

The calculation of the neutron flux produced by an ICF pellet is a problem not often encountered in non-weapons oriented neutronics studies. In particular, the problem involves a background medium with a time varying density. Initially, the pellet is assumed to be in a fully compressed state. As the fuel burns, the outer regions of the target begin expanding. Propagating steadily toward the outer surface of the pellet, the burn front creates regions of reduced ion density due to fuel consumption. In addition, alpha particles produced during the DT reactions are deposited in the pellet and lead to a time

dependent helium buildup. An accurate determination of the emitted neutron spectrum must account for these spatial and temporal ion density variations as well as similar variations in the neutron source.

A time dependent rather than an adiabatic approach is suggested by the results of pellet hydrodynamics calculations. An example of the time dependence of the tritium density in various zones of a pellet ($\rho R$ = 2.98 g/cm$^2$) is shown in Fig. 1. This result has been obtained using the Pellet Hydrodynamics code PHD-IV developed by G.A. Moses and G. Magelssen.[5] In the figure, zone 1 is the core of the pellet ($r_{core}$ = 14.87 μm, $r_{pellet}$ = 89 μm at t=0.0) and zone 10 is the outermost fuel region. Initially, the width of each zone except the first is 8.26 μm. (The hydrodynamics code employs a Lagrangian spatial mesh so the zone sizes change with time.) Note the sudden density changes as the burn front passes through particular zones. Neutrons born early in the burn traverse a significantly different pellet than those born later. In addition, a time of 2.5 ps is required for a 14 MeV neutron to travel a mean chord length of this compressed pellet. Thus, the state of the pellet can change markedly as a neutron passes through. An adiabatic approximation requires time averaging of the densities and sources and we believe this does not accurately represent the true situation.

The code used for the neutron transport calculation is a modified version of TDA. Included in the modifications is the ability to accept new material densities and neutron sources in all spatial intervals at any desired number of time steps. Implicit in the material density input modification is the capacity to add new materials to the pellet as a function of time. The deposition of helium is easily modelled in this manner. Initially the helium is present in all zones but with a density of zero. As the pellet

burns, the density is allowed to increase. This effect is not negligible since the atom density of helium reaches levels that are an order of magnitude higher than the fuel density on the inner zones and up to 20% of the D or T density in the outer zones.

As a concession to computational economics, a spatial mesh fixed to the size of the compressed pellet is used. The actual material densities in an expanding pellet are mapped by transformation onto the fixed spatial grid by preserving the ratio of the interval width to the neutron mean free path. This properly preserves all terms in the transport equation except for the gradient term. However, since most of the neutrons are born before the pellet has expanded appreciably, the error introduced by neglecting the variation of this term is not considered significant. An alternative method is to use an Eulerian spatial grid which extends beyond the imploded pellet radius. As time progresses, the pellet expands through the mesh. This technique, however, is beset by an increase in computer core size required, computing time and cost. The implementation of this method does not appear to be necessary at this time.

The time dependent input data, i.e. density and source spatial profiles, are obtained using PHD-IV. The hydrodynamics code utilizes time steps as small as 0.01 ps which are much too small for practical neutronics calculations. To select the time interval over which to average the data for input to TDA, two criteria are established. The first is that during any time interval, the density in a zone cannot change by more than a factor of two. Secondly, the peak of the neutron source spatial distribution is not allowed to move by more than one zone during a timestep. The second criterion is limiting only at times during the early stages of the burn.

A time interval of 2 ps is found to satisfy both restrictions so this is the interval selected for the input of new data to TDA. To insure convergence and particle balance, the transport time step is 0.5 ps which permits the calculation to proceed for four time steps before accepting new data.

## III. Application and Results

### a) Neutron Spectra and Materials Damage Parameters

Calculations have been performed for three types of pellets. Two are bare, equimolar DT pellets with $\rho R$ values of 3 g/cm$^2$ and 6 g/cm$^2$. The other pellet is an equimolar DT sphere with $\rho R$ = 3 g/cm$^2$ surrounded by a Hg tamper with a $\rho R$ = 8 g/cm$^2$. In all cases the fuel has a radius of 89 μm and in the third example the tamper has a thickness of 20 μm. Initial number densities in the compressed pellets are $N_D = N_T = 4.025 \times 10^{25}$/cm$^3$ and $N_{Hg} = 1.374 \times 10^{25}$/cm$^3$ in the tamped pellet.

The neutron spectra representative of the two bare pellets are contrasted in Fig. 2 with the spectrum calculated neglecting neutron-fuel interactions. The uncollided spectrum is shaped only by Doppler broadening and the directed motion of the exploding fuel particles. The curves are normalized to a pellet energy yield of 100 MJ. General features of the spectra can be divided into three energy ranges. First, the region between 13 and 15 MeV contains the large peak due to uncollided source neutrons escaping the pellet. In a target with $\rho R$ = 3 g/cm$^2$, 76% of the neutrons are uncollided whereas 51% of the neutron population from a pellet with $\rho R$ = 6 g/cm$^2$ escape without interacting. Second, there is a valley bounded by peaks at 2 and 13 MeV in the spectrum. Neutrons are scattered into this region via first group collisions. The differential elastic scattering cross sections for deuterium and tritium have maxima at $\mu_o = \pm 1$, where $\mu_o$ is the cosine of the scattering angle in the center of mass system. This accounts for the local peaking at 2.5 and 3.3 MeV

(noticeable on the $\rho R = 3\ g/cm^2$ curve). The peak at 2.5 MeV is enhanced by neutrons produced from DD reactions. The third distinctive part of the spectrum occurs for neutrons with energy below 2 MeV. Such neutrons are produced by (n,2n) reactions at high energy, multiple elastic scattering of DT fusion neutrons, and elastic scattering of DD fusion neutrons. Multiple elastic scattering is very small for the $\rho R = 3\ g/cm^2$ pellet but significant in the higher density pellet. The major source of neutrons in this region is the (n,2n) reaction with the fuel. The (n,2n) cross section in the first group comprises 13% of the total interaction cross section so that 3% of the DT source neutrons undergo this reaction. The actual increase in neutron population is $\sim$ 4.4% which includes multiplication reactions in lower energy groups, since (n,2n) events are characterized by a large energy loss and lead to a much softer spectrum than is possible to produce by elastic scattering alone.

The tamper surrounding the fuel portion of a pellet affects the spectrum in two ways. By providing an inertial barrier which prevents the immediate expansion of the pellet, the tamper increases the neutron production (more than double in this study) by increasing the time at which the fuel is at a high density. In addition, even though neutrons are not scattered in the tamper (its thickness being $\lambda/40$ where $\lambda$ is the mean free path of a 14 MeV neutron) the probability of multiple scattering in the fuel is increased. This causes additional softening and smoothing of the neutron spectrum. The spectra calculated for a tamped pellet ($\rho R_{fuel} = 3\ g/cm^2$) is shown in Fig. 3.

Spectral softening has a very important impact on radiation damage analysis of the reactor chamber materials. Time dependent displacement rates are examined here since swelling in metals depends not only on the total number of displacement incurred but also on the rate at which the damage is produced.[6] Since the energy spectrum of the neutrons is degraded at a relatively large distance from the first wall, the arrival time distribution of the particles is significantly broadened by time-of-flight. The neutron distribution at the first wall characteristic of a pellet of $\rho R = 3$ g/cm$^2$ is shown in Fig. 4 as a function of time after pellet explosion. The two curves represent the collided and uncollided spectra.

The influence of spectral broadening on displacement rates is evident in Fig. 5. The abscissa in this figure is the time after the leading edge of the neutron pulse strikes the first wall. Note that the displacement rate characteristic of the collided spectrum is broader and has a lower peak than the rate induced by the uncollided distribution.

The spectral softening has a surprising influence on the time integrated damage in a graphite first wall. Since the dpa cross section in graphite has a local maximum at 3.5 MeV, the total number of displacements increases with $\rho R$ for $\rho R$ in the range, 0-6 g/cm$^2$ as used in our investigation. In contrast, helium production decreases as $\rho R$ increases due to the threshold nature of the $(n,\alpha)$ and $(n,3\alpha)$ reactions in graphite. The result will generally be true for all materials except those with significant slow neutron $(n,\alpha)$ cross sections (such as $^{59}$Ni or $^{10}$B). We show in Fig. 6 the result of damage calculations characteristic of a 3000 MW$_{th}$ (100 MJ yield at 30 pellets/sec) fusion reactor with a 6 m radius reaction chamber.

b) Induced Radioactivity in the Target

In a "typical" pellet design, the tamper is optically very thin to

fusion neutrons. However, the neutron flux at the surface of the pellet is high, so that a non-negligible activation of the tamper material can occur. This is crucial to the analysis of chamber gas handling systems and an evaluation of the total radioactivity in a reactor. We consider here the use of an iron tamper and we use the neutron pellet spectrum from the case discussed earlier of a Hg tamper. Radioactivity calculations for the case of a 10 mg Fe tamper were performed using the DKR code developed by Sung and Vogelsang at the University of Wisconsin.[7] It is assumed that each target is fabricated with fresh tamper material.

The results show that the activity generated after one year of operation is 1.35 $Ci/W_{th}$ in a reactor with a target repetition rate of 30 Hz and a target yield of 100 MJ. This radioactivity level is slightly higher than that produced in a 316 SS structural support plate that is 4 cm thick and is located 60 cm behind the first wall in the SOLASE conceptual laser fusion reactor design.[8] (The first 60 cm of blanket is graphite and lithium oxide.) This steel back structure accounts for essentially 100% of the total blanket radioactivity after reactor shutdown out to at least 50 years. As such, we find that the total radioactive inventory in the SOLASE design is doubled if the activation of an Fe tamper is included. Clearly, the magnitude of the effect will depend on the tamper material used. The calculations here point out the importance of considering activation of target materials in ICF reactor design.

## IV. Conclusions

An ICF pellet though very small is not transparent to neutrons. Neutron spectra calculations performed using a modified version of TDA show there is a substantial softening of the spectrum which ultimately manifests itself as a time-of-flight broadening of the arrival time of the neutron

pulse at the first wall. Both the softening and the broadening effects increase with increasing pellet $\rho R$.

Damage calculations for fusion reactors often use an uncollided spectrum. We find that especially for time dependent studies a spectrum which accounts for neutron-pellet interactions should be used. The peak instantaneous dpa rates can be lowered by about 50% when the pellet $\rho R$ is 3 $g/cm^2$. The number of displacements per atom changes by a smaller amount (5-10%) as does the total helium production rate (10-15% decrease). Finally, the amount of radioactivity generated in target tamper materials can equal or exceed total radioactivity generated in the rest of the reactor system.

Acknowledgement

Support for this work has been provided by the United States Department of Energy, Office of Laser Fusion.

## References


1. F.H. Southworth and J.D. Campbell, "Neutron Downscattering in Dense Fusioning Plasmas", Trans. Amer. Nucl. Soc. 21 (1975) 15.

2. T.D. Beynon and G. Constantine, "Energy Deposition by Fast Neutrons in Laser Compressed D-T Pellets", J. Phys. G: Nuclear Physics 1 (1975) L23.

3. J.A. Blink, P.E. Walker, H.W. Meldner, "Energy Partition and Neutron Spectra from Laser Fusion Reactor Targets", Trans. Amer. Nucl. Soc. 27 (1977) 70.

4. S.A. Dupree, et al., "Time Dependent Neutron and Photon Transport Calculations Using the Method of Discrete Ordinates", Joint Los Alamos Scientific Laboratory - Oak Ridge National Laboratory Report LA-4557 (ORNL-4662) (1971).

5. G.A. Moses and G. Magelssen, "PHD-IV, A Plasma Hydrodynamics - Thermonuclear Burn - Radiative Transfer Computer Code", Nuclear Engineering Department Report UWFDM-194, University of Wisconsin (1977).

6. N. Ghoniem and G.L. Kulcinski, "Swelling of Metals Under Pulsed Irradiation", Nuclear Engineering Department Report UWFDM-179, University of Wisconsin (October 1976).

7. T.Y. Sung and W.F. Vogelsang, "DKR: A Radioactivity Calculation Code for Fusion Reactors", Nuclear Engineering Department Report UWFDM-170, University of Wisconsin (September 1976).

8. R.W. Conn, et al., "SOLASE - A Conceptual Laser Fusion Reactor Design", Nuclear Engineering Department Report UWFDM-220, University of Wisconsin (December 1977).

## FIGURE CAPTIONS

Fig. 1 Tritium density in various zones of an ICF pellet as a function of time after initiation of central thermonuclear burn.

Fig. 2 The neutron spectrum from a bare ICF target as a function of the $\rho R$ value at initiation of burn. $\rho R=0$ is taken to represent the case where neutron interactions with the pellet are neglected.

Fig. 3 The neutron spectrum from a tamped ICF target (Hg is used as the tamper).

Fig. 4 Arrival time of fusion neutrons at a first wall that is 6 m from the target. Doppler broadening is included in both cases.

Fig. 5 The difference in a primary first wall damage indicator (dpa/sec) depending upon whether collisions of neutrons with the pellet during burn are included.

Fig. 6 The change in first wall dpa and He production rates as a function of target $\rho R$ at initiation of burn. Both Doppler and collisional broadening of the neutron spectrum are included.

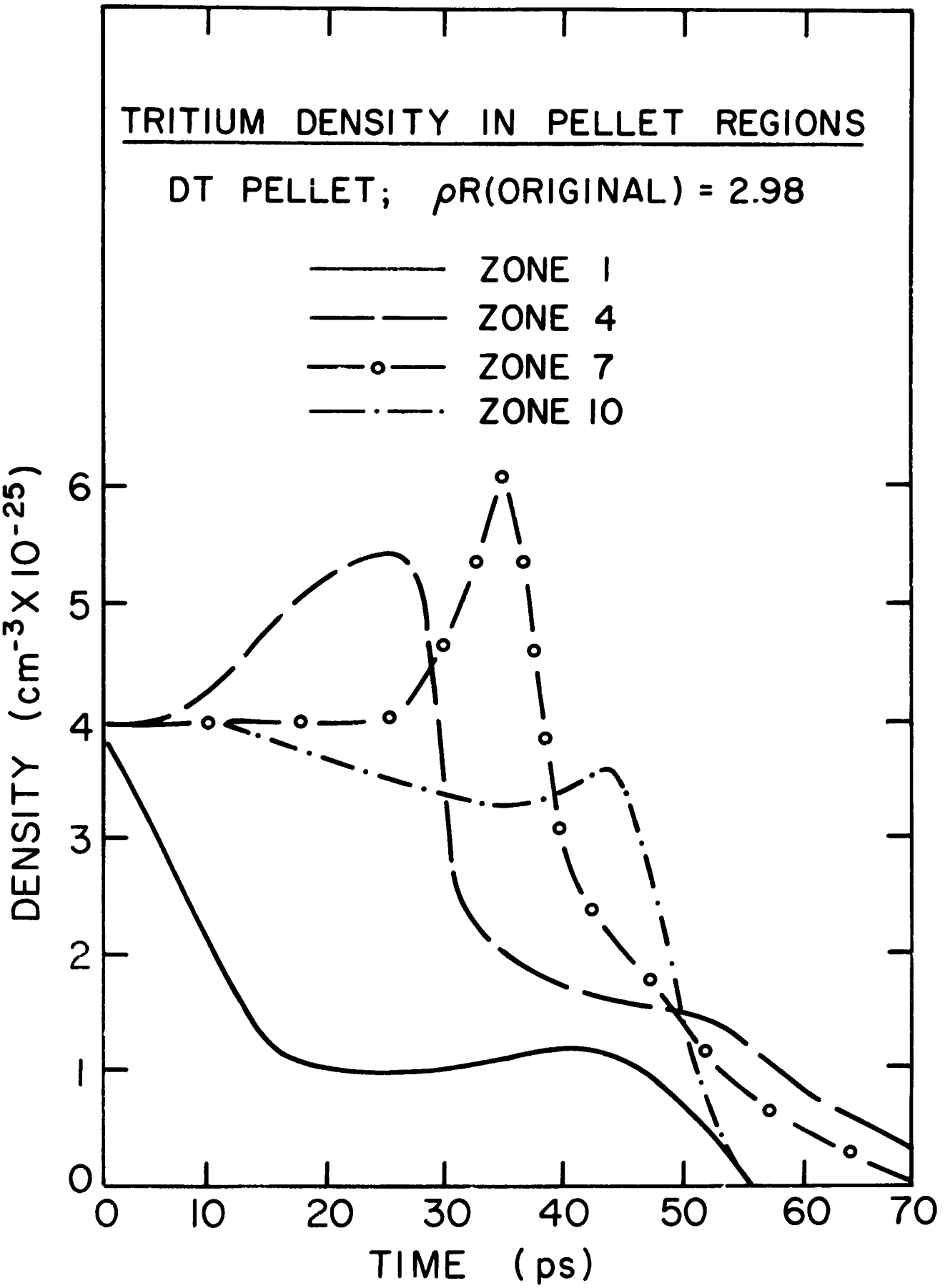
TRITIUM DENSITY IN PELLET REGIONS
DT PELLET; ρR(ORIGINAL) = 2.98
ZONE 1
ZONE 4
ZONE 7
ZONE 10
DENSITY (cm⁻³ X 10⁻²⁵)
0
1
2
3
4
5
6
0
10
20
30
40
50
60
70
TIME (ps)

Figure 1

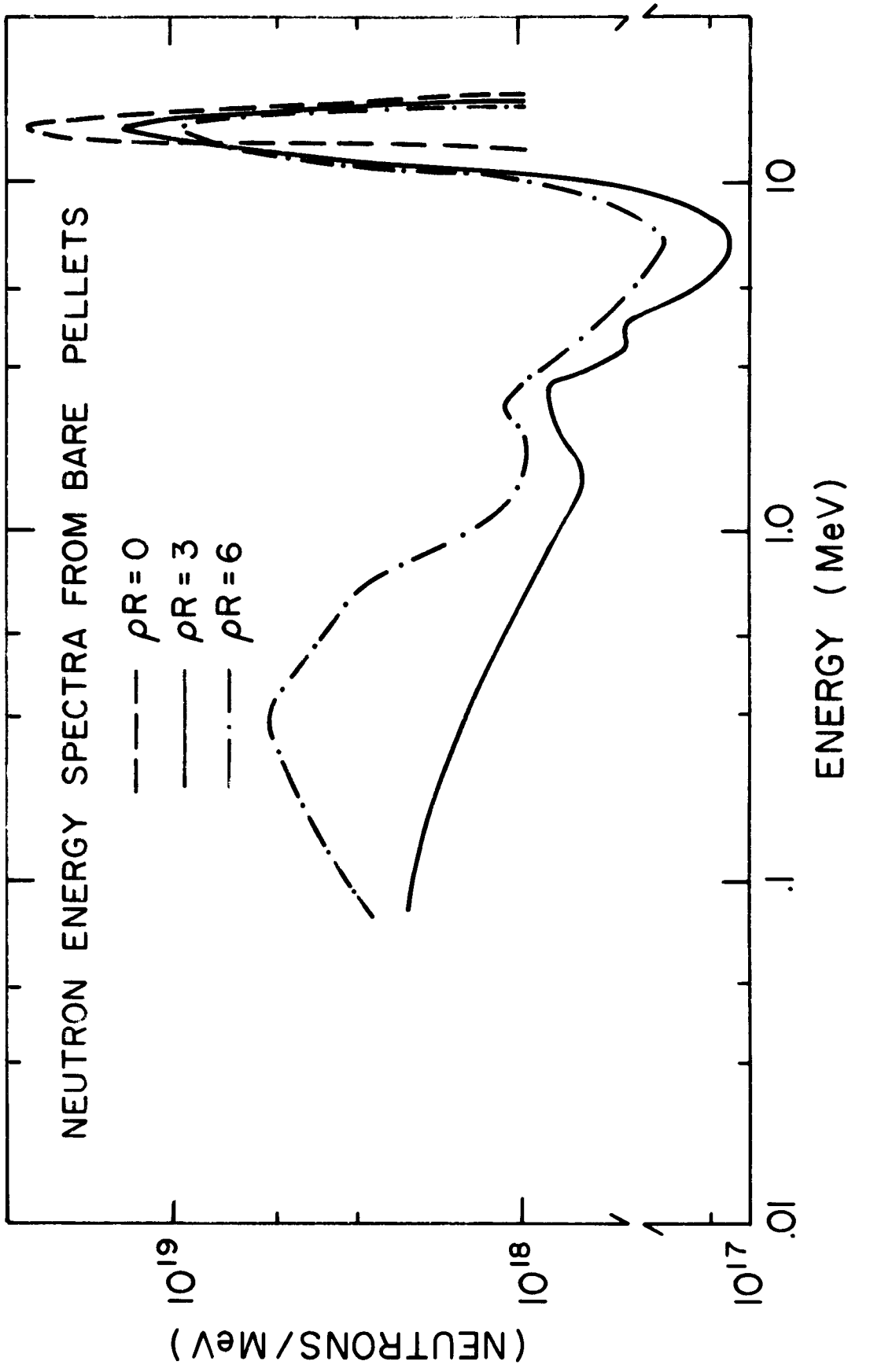
NEUTRON ENERGY SPECTRA FROM BARE PELLETS
ρR = 0
ρR = 3
ρR = 6
(NEUTRONS/MeV)
10^19
10^18
10^17
.01
.1
1.0
10
ENERGY (MeV)

Figure 2

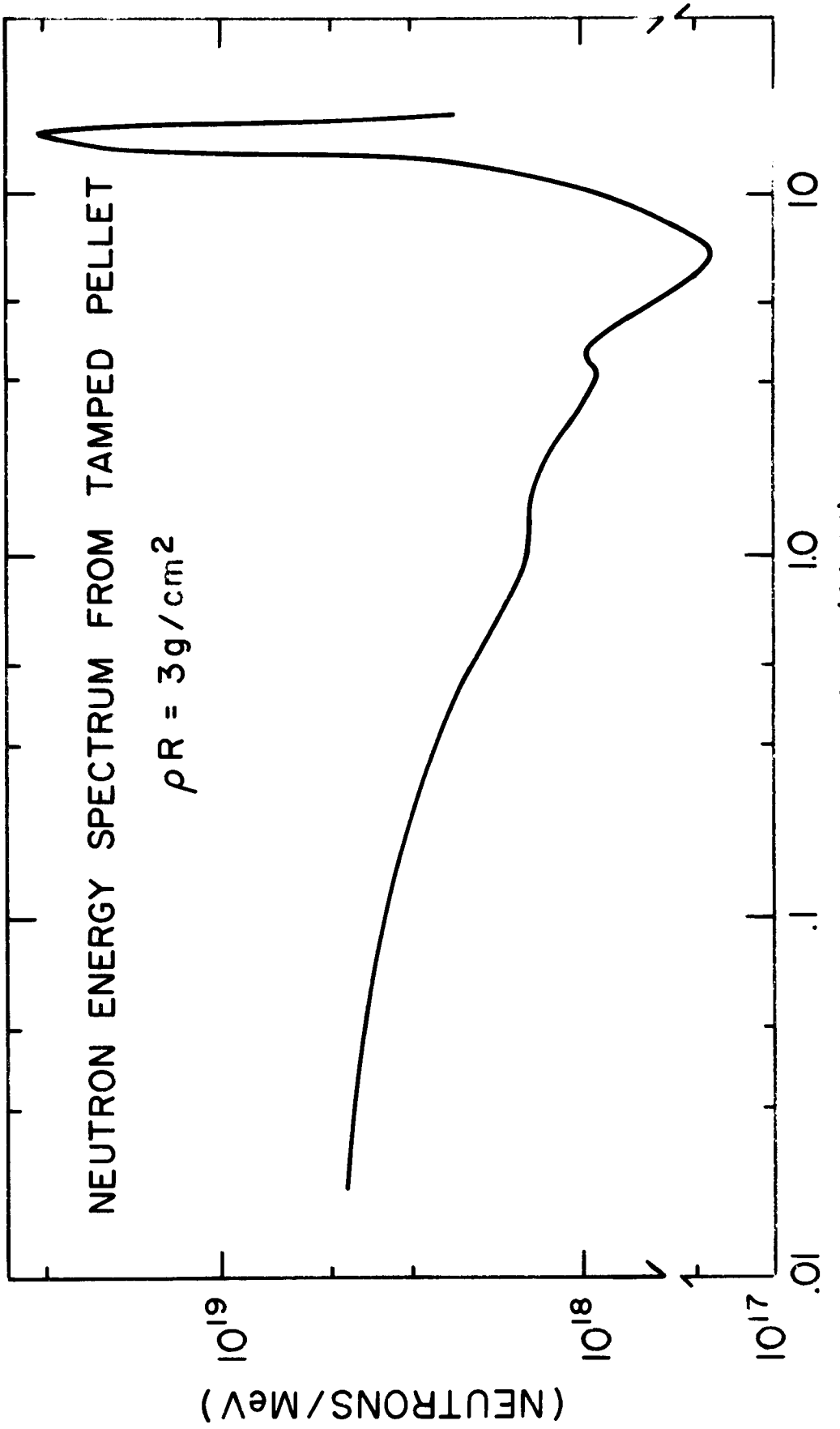
NEUTRON ENERGY SPECTRUM FROM TAMPED PELLET
ρR = 3g/cm²
(NEUTRONS/MeV)
10¹⁹
10¹⁸
10¹⁷
.01
.1
1.0
10
ENERGY (MeV)

Figure 3

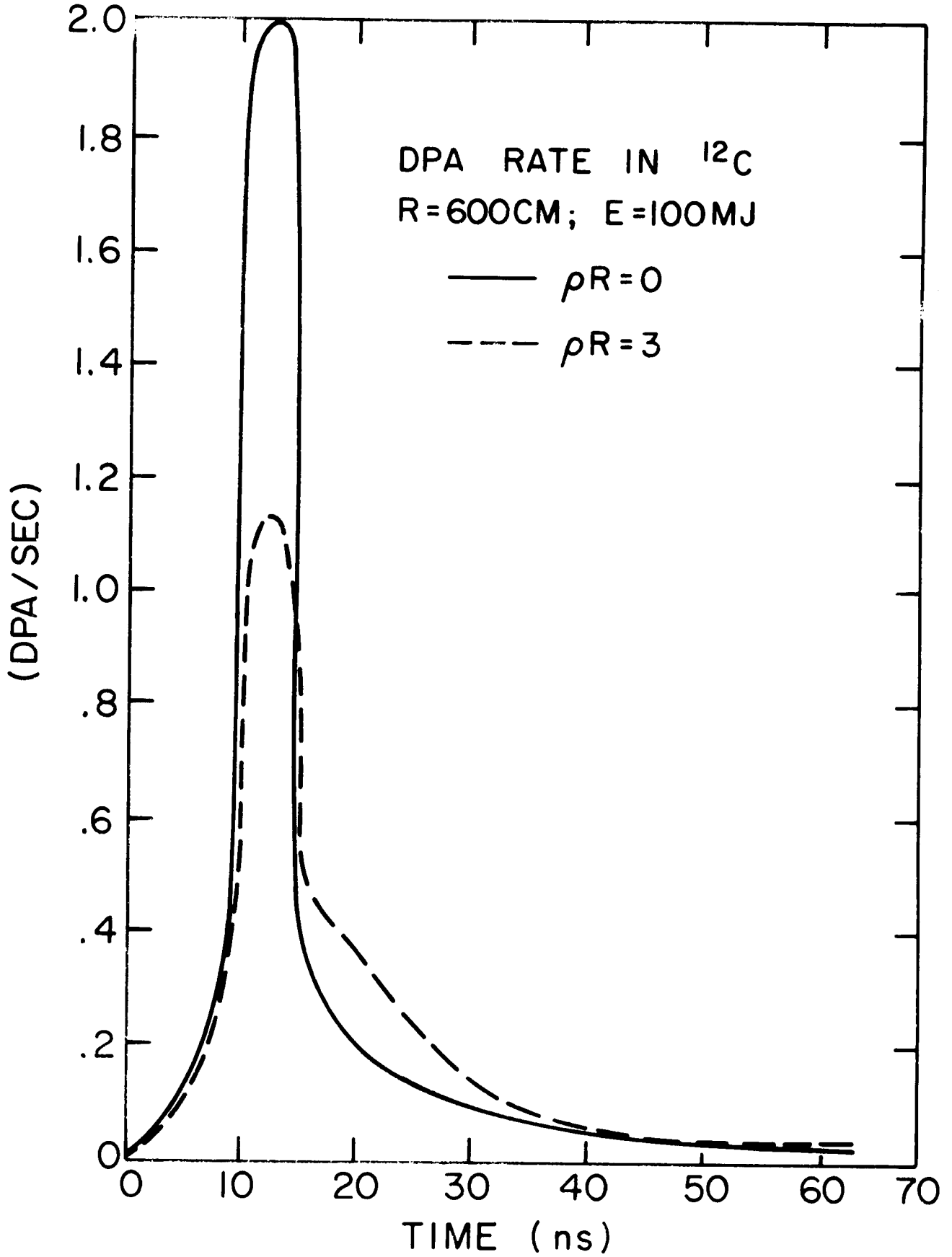
DPA RATE IN $^{12}C$
R=600CM; E=100MJ
$\rho R=0$
$\rho R=3$
(DPA/SEC)
TIME (ns)
2.0
1.8
1.6
1.4
1.2
1.0
.8
.6
.4
.2
0
0
10
20
30
40
50
60
70

Figure 5

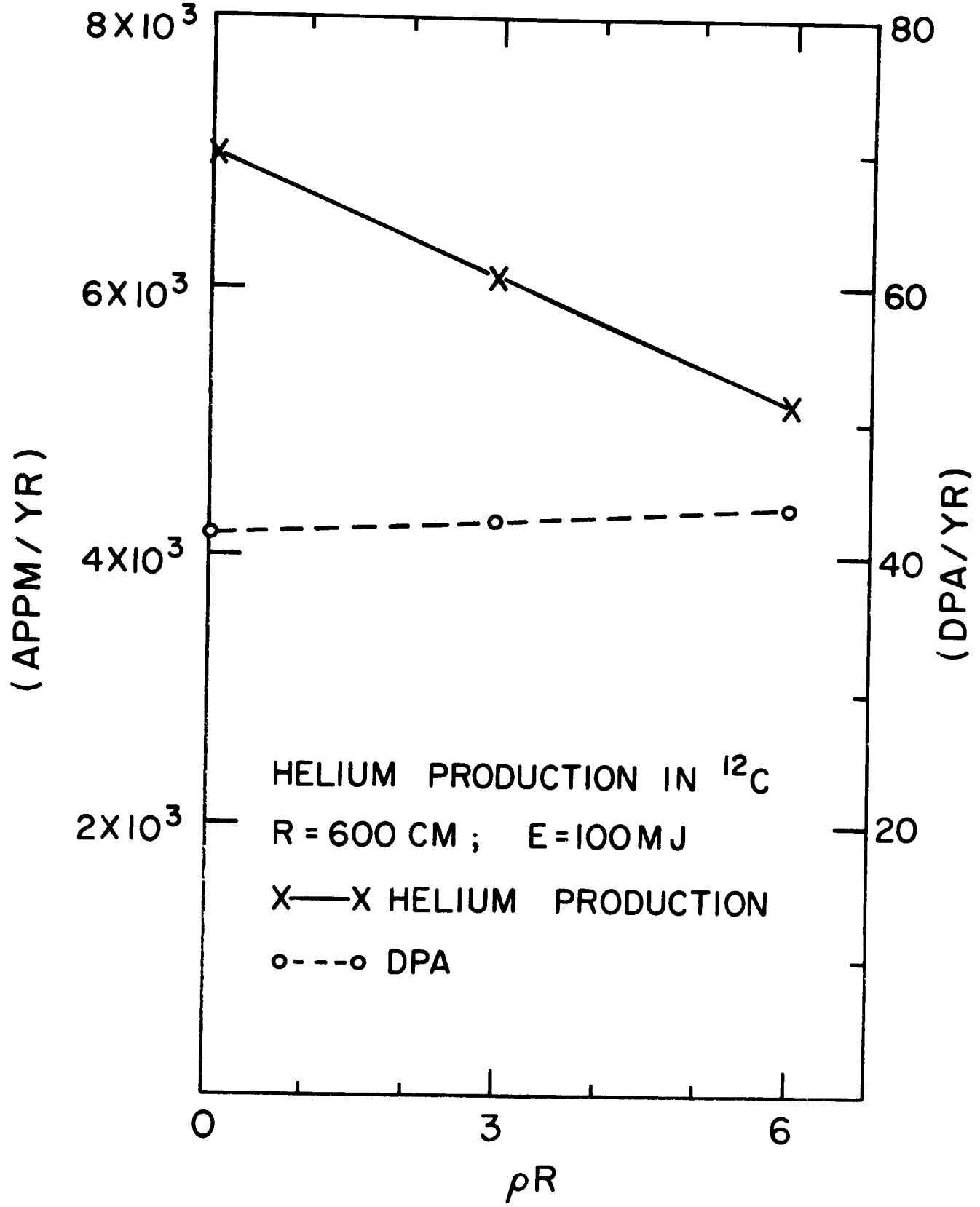
8X10³
6X10³
4X10³
2X10³
80
60
40
20
(APPM/YR)
(DPA/YR)
HELIUM PRODUCTION IN ¹²C
R = 600 CM ; E = 100 MJ
X—X HELIUM PRODUCTION
o---o DPA
0
3
6
ρR

Figure 6